

ESTIMATION OF GLOBAL ANNUAL RIVER RUNOFF BASED ON ATMOSPHERIC WATER BALANCE

BY

Taikan OKI, Katumi MUSIAKE

Institute of Industrial Science, University of Tokyo,
Roppongi, Minato-ku, Tokyo 106, Japan

and

Kooiti MASUDA

Department of Geography, Tokyo Metropolitan University,
Minami-Osawa, Hachioji, Tokyo 192-03, Japan

SYNOPSIS

The global distribution of vapor flux convergence $-\nabla_H \cdot \vec{Q}$ is estimated using the ECMWF (European Centre for Medium-Range Weather Forecasts) global analysis data for the period from 1985 to 1988. The $-\nabla_H \cdot \vec{Q}$ can be interpreted as the precipitation minus evaporation in the annual water balance.

The zonal mean of the calculated vapor flux convergence shows good correspondence with prior estimations. The $-\nabla_H \cdot \vec{Q}$ is also compared with the runoff of large rivers. The multi-annual mean of the GRDC (Global Runoff Data Centre) data set is used for the comparison. The mean runoff of the GRDC rivers is approximately 310 mm/year, and the vapor convergence value by this study for the GRDC river basins is 220 mm/year. The difference probably due to weakness of the convergence (or divergence). Similarly, the global annual river discharge from the continents to the sea should also be higher than 170 mm/year, value obtained by total flux convergence over whole land.

Good relationships are observed between atmospheric water balance and the runoff observations at the ground, especially in the northern hemisphere. The authors consider that this result indicates the importance of daily atmospheric observations and accurate observations of the river discharges. The method presented here is expected to be the most useful in estimating the global water balance and the availability of global water resources.

INTRODUCTION

There are three research topics to be investigated by hydrologists addressing problems of global change :

- (i) better understanding of the reality and the mechanism about global water circulation and balance;
- (ii) the development of climate models which can represent the regional scale water circulation and balance, including precise hydrological surface models at GCM(general circulation model) grid scales;
- (iii) the interpretation of the model forecast for social activities.

The first research topic is resolving the problem and enrich the knowledge of global hydrology. Such research will contribute to the effective display of global hydrological data for use in the validation of climate simulations. The deeper understanding of the global water circulation and its variability would also permit forecasting of the long term water resources changes. Therefore it is still important in water

resources engineering to investigate the global water cycle and balance, and to examine them in the river basin scale.

The second research topic concerns expansion of the spatial scale of hydrological models, which would be the traditional problem in hydrological science. The GCM-grid-size hydrological model with a spatial scale of approximately 100km is currently employed to represent land surface processes of the GCMs. There have already been such models which include soil and vegetation, heat and water balance and radiative transfer processes. However one does not know which model performs well or what model, because there have been few validations of the data and methods. A critical problem is how to define and measure the surface soil moisture content at the scale of 100km scale grid cell.

Urgent social needs surrounding topic (iii) have led to some investigations concerning water resource changes in river basins for various global climate change scenarios. Hydrologist should extend such research field in a continuing effort to answer the social needs. This research may at times require hydrologists to forecast the global change.

This study focuses on the first topic. River runoff (= precipitation – evaporation) is estimated using global atmospheric data by atmospheric water balance method. The annual global value of river runoff, the latitudinal distribution and the annual river runoff in each large river basin are presented. The results and the method presented here will contribute to the method from the basin scale to the global scale.

GLOBAL WATER BALANCE

The water balance at the global scale is a traditional topic in geographical hydrology and has been estimated in numerous studies. Korzun [3] summarized such results, which were obtained by observations of precipitation and runoff at the ground, and calculated evaporation rates using climatological data for temperature over oceans.

Improved computational capabilities now enable large data sets to be effectively processed, and the atmospheric water balance method, first used by Starr [7], was applied to global water balance estimation by Bryan and Oort [2] and Masuda [5]. The present study employs this method to estimate large scale water balance, and the results are validated using the runoff data observed at the ground surface.

The atmospheric water balance is described by the equation,

$$\frac{\partial W}{\partial t} + \frac{\partial W_c}{\partial t} = -\nabla_H \cdot \vec{Q} - \nabla_H \cdot \vec{Q}_c + (E - P), \quad (1)$$

where, W , W_c , \vec{Q} , \vec{Q}_c , E , P represent precipitable water(column storage of water vapor), column storage of liquid and solid water, vertically integrated two dimensional vapor flux, vertically integrated two dimensional water flux in liquid and solid phase, evaporation, and precipitation, respectively. The term ∇_H represents the horizontal divergence. The water balance of a river basin is described as,

$$\frac{\partial S}{\partial t} = -\nabla_H \cdot \vec{R}_o - \nabla_H \cdot \vec{R}_u - (E - P), \quad (2)$$

where S represents the storage in the basin, and \vec{R}_o and \vec{R}_u represents surface runoff and the ground water movement, respectively.

The following assumptions are employed in annual water balance computations.

- (i) Annual change of atmospheric vapor storage is negligible (left hand side of the equation (1) is equal to 0).
- (ii) advection of water in liquid and solid phase (\vec{Q}_c) is negligible in large scale(ex., 2.5° global mesh).
- (iii) Annual change of basin water storage ($\frac{\partial S}{\partial t}$) is negligible and all ground water movement is observed at the gauging point of the river used here($\nabla_H \cdot \vec{R}_u = 0$).

With these assumptions, equation (1) and equation (2) is simplified to

$$-\nabla_H \cdot \vec{Q} = (P - E) = \nabla_H \cdot \vec{R}_o. \quad (3)$$

In this simplified equation, the water vapor convergence, (precipitation – evaporation) and runoff of that area are equal in the annual water balance. The global annual runoff is examined below based on this equation.

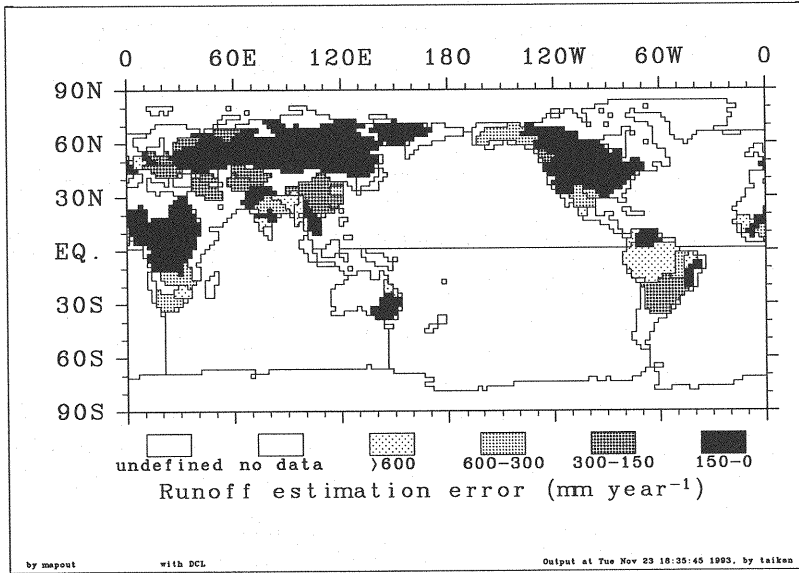


Figure 1: Land-sea distribution and river basins. The absolute difference between vapor flux convergence and river runoff are indicated.

DATA ANALYSIS

Data Description

The atmospheric data used in this analysis is from the ECMWF (European Centre for Medium-Range Weather Forecasts) objective analysis data made through 4-dimensional assimilation system. River runoff observed at the ground is from GRDC(Global Runoff Data Centre) and also from values reported by UNESCO [8]. Thirty five rivers which have basin areas greater than approximately 300,000 km² were selected. A global elevation data set on a 2.5° grid was also made, and the Continents of the globe were divided into river basins(Fig.1).

ECMWF data processing

Wind(u, v), temperature(T), relative humidity(R_H) and pressure height(Z) are given in seven levels corresponding to 1000, 850, 700, 500, 300, 200, 100 hPa within the 2.5° global grid cells. Relative humidity is defined only for the lower five pressure levels. The data for the period from 1985 to 1988 is used here considering the homogeneity of the quality [6], and the time interval of the data is twice daily. The algorithm to estimate the $-\nabla_H \cdot \vec{Q}$ is described in this section.

(a) Surface pressure

For consistency in data handling, extrapolated values are stored at pressure levels under ground surface. It occurs when the surface pressure is below 1000 hPa, and sometimes below 850/700 hPa in mountainous regions. Surface pressure is also necessary for the vertical integration, and requires computation in a manner similar to the reduction to mean sea level;

- (i) The tentative mean temperature between 1000[hPa] and ground surface is computed, using the temperature ($T_{1000}[^{\circ}\text{C}]$) and pressure height ($Z_{1000}[\text{gpm}]$) at the lowest level of the data. The

equation is

$$T_m = T_{1000} + \Gamma(Z_{1000} - Z_h), \quad (4)$$

where Z_h [m] is the altitude at that grid, and adiabatic temperature lapse rate Γ is set to $0.005[^\circ\text{C}/\text{m}]$.

(ii) A temperature correction factor ε_m that takes into account moisture effects is computed as

$$\varepsilon_m = \begin{cases} 0.0, & T_m \leq -20.0 \\ \frac{3}{55}(T_m + 20.0), & -20.0 \leq T_m \leq 35.0 \\ 3.0, & 35.0 \leq T_m \end{cases} \quad (5)$$

The corrected mean temperature T'_m [K] is computed according to the equation $T'_m = 273.15 + T_m + \varepsilon_m$.

(iii) Surface pressure P_s is given using the lowest pressure P_{1000} , gas constant $R_d (=287.05 \text{ [m}^2/\text{s}^2\text{K]})$, and the gravity constant $g (=9.80 \text{ [m/s}^2\text{]})$:

$$P_s = P_{1000} e^{\frac{g(Z_h - Z_{1000})}{R_d T'_m}}. \quad (6)$$

(b) Values at ground surface

Physical values at ground surface A_s is interpolated using values A_k and A_{k+1} at the levels of P_k and P_{k+1} ($P_k \leq P_s \leq P_{k+1}$). $P_k=1000$ [hPa] and $P_{k+1}=850$ [hPa] are used for extrapolation in case of $P_s \leq 1000$ [hPa]. Logarithmic values of pressure is used for interpolation (or extrapolation). The equation is defined as

$$A_s = A_k + (A_{k+1} - A_k) \frac{\log P_s - \log P_k}{\log P_{k+1} - \log P_k}. \quad (7)$$

(c) Specific humidity

Specific humidity can be computed using the pressure p , temperature T [K], and relative humidity R_h [%], according to the equation

$$q = \frac{\varepsilon \frac{R_h}{100} e_s(T)}{p - (1 - \varepsilon) \frac{R_h}{100} e_s(T)}, \quad (8)$$

where $\varepsilon (\approx 0.622)$ is the ratio of the density between dry air and the water vapor. Saturated vapor pressure $e_s(T)$ [hPa] at temperature T [K] is calculated using Gratch's equation:

$$\begin{aligned} \log_{10} e_s &= 10.79574 \left(1 - \frac{T_1}{T}\right) - 5.02800 \log_{10} \left(\frac{T}{T_1}\right) \\ &+ 1.50475 \times 10^{-4} \left\{1 - 10^{-8.2969 \left(\frac{T}{T_1} - 1\right)}\right\} \\ &+ 0.42873 \times 10^{-3} \left\{10^{4.76955 \left(1 - \frac{T_1}{T}\right)} - 1\right\} + 0.78614. \end{aligned} \quad (9)$$

$T_1 (=273.16 \text{ [K]})$ is the triple equilibrium temperature of water, and the saturated vapor pressure for liquid water surface is also used in case $T < 0[^\circ\text{C}] = 273.15 \text{ [K]}$.

(d) Vertical Integration and Horizontal Convergence

The vertical integration of $W = \int_0^{p_s} q \frac{dp_i}{g}$ is computed as $W = \frac{1}{g} \sum_{i=1}^7 q_i \delta p$. The thickness of the layer δp_i is given by

$$\delta p_i = \begin{cases} 0.0, & p_i < p_s \\ \frac{p_i - p_{i+1}}{2}, & p_i = p_s \\ \frac{p_{i-1} - p_{i+1}}{2}, & p_s < p_i, \quad 1 < i < 7 \\ \frac{p_6 - p_7}{2}, & i = 7 \end{cases} \quad (10)$$

The components of the 2-dimensional vapor flux $\vec{Q} = (Q_\lambda, Q_\phi)$, $Q_\lambda \equiv \int_0^{p_s} qu \frac{dp}{g}$ and $Q_\phi \equiv \int_0^{p_s} qv \frac{dp}{g}$ are similarly computed. Horizontal vapor flux divergence is given as

$$-\nabla_H \cdot \vec{Q} = -\frac{1}{a \cos \phi} \left\{ \frac{\partial Q_\lambda}{\partial \lambda} + \frac{\partial Q_\phi \cos \phi}{\partial \phi} \right\}, \quad (11)$$

where $a(\approx 6,360 \text{ [km]})$ is the radius of the earth, and ϕ is the latitude at the point. In the discrete equation, the convergence $-\nabla_H \cdot \vec{Q}[i, j]$ at latitude of $\lambda[i]$ and longitude of $\phi[j]$ can be written:

$$-\nabla_H \cdot \vec{Q}[i, j] = \frac{Q_\lambda[i+1, j] - Q_\lambda[i-1, j]}{a \cos(\phi[j])(\lambda[i+1] - \lambda[i-1])} + \frac{\cos(\phi[j+1])Q_\phi[i, j+1] - \cos(\phi[j-1])Q_\phi[i, j-1]}{a \cos(\phi[j])(\phi[j+1] - \phi[j-1])}. \quad (12)$$

Vapor flux convergence is given with dimensions of $[\text{kg/m}^2\text{s}]$, and is converted into $[\text{mm/year}]$ by assuming the density of water to be $1.0[10^3\text{kg/m}^3]$, which simplifies the comparison with annual runoff.

Table 1: Estimates of Global Annual Runoff from Whole Continents (mm/year) from previous studies and from the present study.

269	Lvovitch[4]	Basin water balance
256	Baumgartner & Reichel[1]	Basin water balance
303	Unesco[3]	River runoff
42	Bryan & Oort[2]	Atmospheric water balance, 1963-1974
152	Masuda[5]	ECMWF data, year of FGGE(1979)
260	Masuda[5]	GFDL data, year of FGGE(1979)
167	This study	ECMWF data, 1985-1988

RESULTS

Global Annual Runoff from Whole Continents

Global annual runoff from whole continents is calculated using the land-sea distribution (Fig. 1) and compared with existing estimates (Table 1). The results of this study are comparable to these with FGGE-ECMWF, and relatively small compared with results by basin water balance. According to Unesco [3], land cover on the earth is approximately 29%, but 31% is assumed in the model employed in this study. The difference between $-\nabla_H \cdot \vec{Q}$ and river runoff in Table 1 may be caused by a bias from weak divergence of the wind in the ECMWF objective analysis data set [5].

Latitudinal Distribution of Global Runoff

Fig. 2 shows the zonal (east-west direction) mean of vapor flux convergence, and the comparison with prior result about the latitudinal distribution of (precipitation - evaporation). They have good agreement quantitatively, but the results of this study shows that evaporation excess over precipitation at sub-tropical latitude is greater than the result by Baumgartner and Reichel [1].

Comparison between vapor flux convergence and river runoff

Annual vapor convergence is estimated in each river basin listed in Table 2. The comparison with observed river runoff is shown in Fig. 3 using the index of the absolute difference between them. If the estimation error is evaluated in the ratio to the observed value, as seen in the last column of Table 2, the ratio of the error (expected to be zero) is roughly within the range of ± 1.0 . This index is, however, not adequate for rivers with small annual runoff because the error may be too significant.

The major difficulties confronted in the comparison of atmospheric vapor convergence and river runoff here are:

- (i) Flux convergence is computed for whole basin in the model topography, but runoff observation points not always represent the whole basin runoff (see Nile or Niger).
- (ii) There are some limit to keep accuracy of the template that divides the continents into river basins. In case of small rivers, it is very hard to define river basin accurately by 2.5° grid.

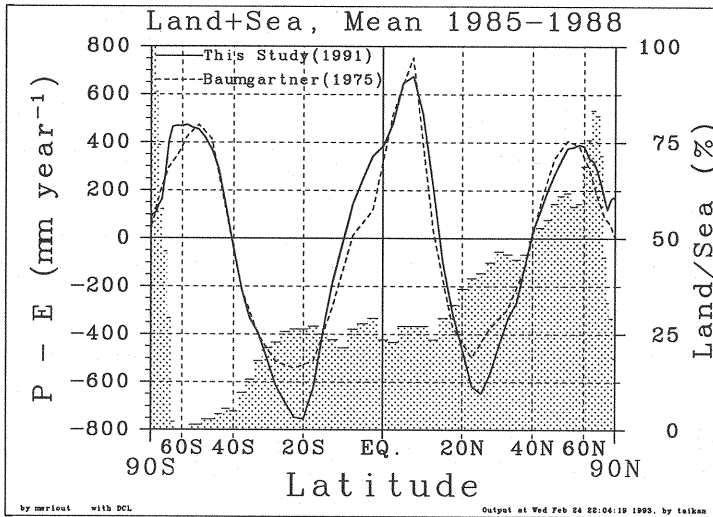


Figure 2: Latitudinal distribution of global runoff. Shadow columns show the percentage of land in each latitude.

- (iii) The observation periods for atmospheric data and runoff are completely different.
- (iv) Quality of runoff observation at each observation point is not known, it may be different each other.

The atmospheric vapor flux convergence and river runoff correspond well, even though their data sources, and temporal and spatial scales are completely different.

The classification of the correspondence between the vapor convergence and the river runoff is shown in Fig. 1. There are good correspondences in the mid and high latitude regions of the northern hemisphere. This distribution may reflect the high quality and high density of the observations, especially with respect to the atmosphere, which underscores the importance of actual observations for accurate data assimilations.

Normalizing for basin area, the mean $-\nabla_H \cdot \vec{Q}$ from these 35 rivers is approximately 220 [mm/year]. This value is larger than that for whole continents, but smaller than the mean runoff of the rivers, which is 314 [mm/year] by GRDC, and 365 [mm/year] by UNESCO. These 35 river basins cover less than half of the land on the earth, yet their mean runoff is larger than global average, which indicates that the areas where large river exists have comparatively high runoff rates. It suggests the global water balance estimated by the extrapolation of the large river water balance may over estimate.

SUMMARY

- (1) The algorithm to compute the vapor flux convergence using the global atmospheric data is shown. The result can be treated as the runoff from the area estimated using the water balance equation.
- (2) Global annual runoff on the earth is estimated to be 167 mm by the ECMWF 4-dimensional assimilation data year of 1985-1988. This value is slightly less than the results from traditional basin water balance. With the exception of the sub tropics, the latitudinal distribution of global runoff corresponds well with previous studies.
- (3) Comparison between vapor convergence and river runoff of 35 large rivers have been made and exhibits strong agreement, especially in mid and high latitudes of the northern hemisphere.
- (4) To our knowledge, this is the first study to employ 4-dimensional assimilation global data in estimating the world water balance, treating land and ocean separately and making comparison in more than 30 large river basins of the globe.

Table 2: Large Rivers in the world and Annual Runoff

River	Area 10^3km^2	Station (GRDC)	Area 10^3km^2	GRDC	UNESCO (mm/year)	$-\nabla_H \cdot \vec{Q}$	$\frac{-\nabla_H \cdot \vec{Q}}{\text{GRDC}} - 1$
Amazonas	6150	Obidos	4640	1057	1176	206	-0.805
Congo(Zaire)	3690	Brazzaville	3475		367	247	-0.326
Mississippi	3248	Alton(III)	444	205	186	114	-0.447
Nile	3007	Khartoum	325	150	159	554	2.705
Ob	2948	Salekhard	2950	134	130	106	-0.212
Yenisey	2592	Igarka	2440	223	230	219	-0.016
Lena	2384	Kusur	2430	216	212	192	-0.110
Parana	2270	Corrientes	1950	264	382	484	0.833
Niger	2092	Koulikoro	120	376	109	-70	-1.186
Amur	2052	Komsomolsk	1730	178	188	119	-0.332
Changjiang	1809	Datong	1705	431	(503)	627	0.455
Mackenzie	1668	Norman wells	1570	168	160	245	0.454
Volga	1420	Volgograd	1360	184	181	99	-0.460
Zambeze	1330	Matundo-Cais	940	112		-283	-3.522
St.Lawrence	1248	Cornwall	774	323	290	315	-0.025
Ganges	1100	Paksey	847		434	-68	-1.156
Murray	1080	Lock9 Upper	991	8		-34	-5.185
Nelson	1060	Bladder Rapids	1000	76	92	176	1.323
Indus	960	Kotri	832	92		-124	-2.349
Orinoco	944	Musinacio	787		935	373	-0.601
Yukon	900	Carmacks	818	35	255	513	13.620
Danube	817	Ceatal Izmail	807	253	244	124	-0.509
Mekong	800	Mukdahan	391		693	914	0.320
Al-Furat	765	Hindiya	274		69	36	-0.473
Huanghe	752	Sanmenxia	688	6	(63)	-235	-42.810
Brahmaputra	660	Pandu	405	1535	998	481	-0.687
Sao Francisco	660	Traipu	623	13	194	-748	-56.558
Columbia	655	TheDalles,Oreg	614	272	284	183	-0.329
Kolyma	630	Sredne-kolymsk	361	192	196	260	-0.351
Colorado	590	Lim.Inte.Norte	632	4	19	-60	-17.525
Dniepr	510	Dniepr	463	101	93	106	0.046
XiChiang	437	Wuzhou	330	681	(682)	46	-0.932
Northern Dvina	362	Ust-Pinega	348	302	306	303	0.002
Magdalena	240	Calamar	257	856	1115	3987	3.655
Fraser	220	Hope	217	397	418	712	0.794

(Basin areas are completely different in each literature)

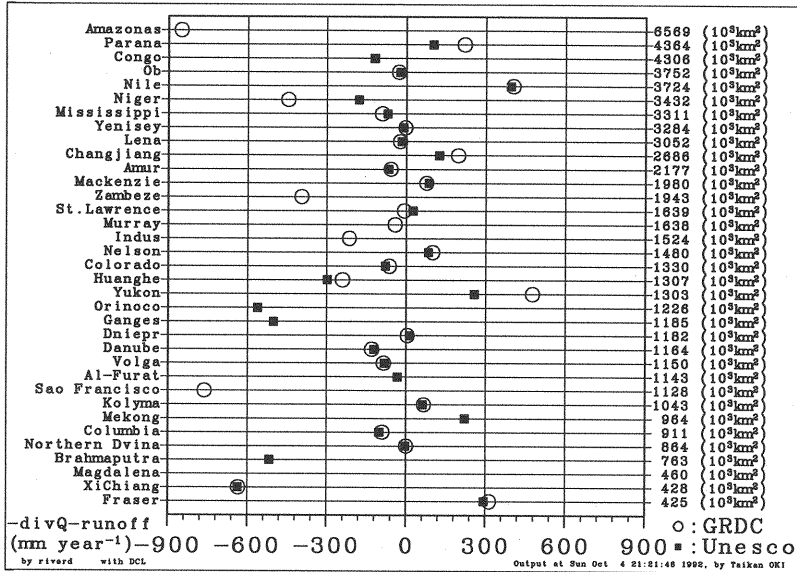


Figure 3: Difference between $-\nabla_H \cdot \vec{Q}$ and river runoff by GRDC or Unesco

ACKNOWLEDGMENTS

The authors wish to thank GRDC for providing precious data sets. ECMWF data set used here is that of Center for Climate System Research, University of Tokyo. We also wish to thank H. Matsuyama, in Department of Geography, Tokyo Metropolitan University, for his very significant contributions to make the global river basin template.

References

- [1] Baumgartner, F., and E. Reichel. *The World Water Balance : Mean Annual Global, Continental and Maritime Precipitation, Evaporation and Runoff*. Ordenbourg, München, 1975. pp.179.
- [2] Bryan, F., and A. Oort. Seasonal variation of the global water balance based on aerological data. *J. Geophys. Res.*, 89, pp.11717-11730, 1984.
- [3] Korzun, V. I., ed. *World Water Balance and Water Resources of the Earth*, volume 25 of *Studies and Reports in Hydrology*. UNESCO, 1978.
- [4] Lvovitch, M. I. The global water balance. *Trans. Am. Geophys. Union*, 54, pp.28-42, 1973.
- [5] Masuda, K. World water balance; analysis of FGGE IIIb data. In J. S. Theon and N. Fugono, editors, *Tropical Rainfall Measurements*, pp.51-55. A. Deepak Publ., 1988.
- [6] Oki, T., K. Musiakke, and H. Siigai. Water balance using atmospheric data — a case study of Chao Phraya river basin, Thailand —. In *Mitteilungsblatt des Hydrographischen Dienstes in Österreich*, volume 65/66, pp.226-230, Wien, 1991.
- [7] Starr, V. P. and J. Peixoto. On the global balance of water vapor and the hydrology of deserts. *Tellus*, 10, pp.189-194, 1958.
- [8] UNESCO, ed. *Discharge of Selected Rivers of the World*, volume I, II, III. UNESCO, 1969.

(Received November 20, 1992 : revised June 9, 1993)